

# An Improved Topology for Multi-pulse AC/DC Converters within HVDC and VFD Systems: Operation in Degraded Modes

D. L. Mon-Nzongo, Student Member, IEEE, P. G. Ipoum-Ngome, Tao Jin, Member, IEEE, and J. Song-Manguelle, Senior Member, IEEE

**Abstract**— An improved topology for a multi-pulse AC/DC converter-based on 6-pulse rectifier modules operating in a degraded mode is described. Its main application is HVDC and VFD systems, where reliability, availability, and maintainability are the most critical requirements. A new concept called, “three-phase electronic Z/z transformers,” which provides separated voltages with reconfigurable phase-shifting angles and voltage ratios, is discussed. The number of acceptable faulty rectifier modules is defined at the design stage. Such features enable AC/DC rectifier systems to be modular and reconfigurable. In contrast with conventional topologies, the proposed structure can operate optimally as an 18-pulse, 12-pulse, or 6-pulse rectifier in faulty conditions of local transformers or rectifier modules. An implementation method for a degraded 24-pulse rectifier with its control architecture including the Z/z transformers’ command unit is discussed. A 1.5 kV, 18 kVA, 18-pulse AC/DC converter associated with a real-time system control is designed and tested. Promising results validate the new concept.

**Index Terms**— Multi-pulse AC/DC converter, HVDC, VFD, reliability, degraded mode, electronics Z/z transformer.

## I. INTRODUCTION

RELIABILITY, availability and maintainability (RAM) of high-voltage DC (HVDC) transmission and variable frequency drive (VFD) systems are the key criteria to effectively secure the global demand for the generation of electric power [1] - [3]. In these systems, the load commutated converter (LCC) technology for very high-power AC/DC and DC/AC conversion not only provides pulsating DC or AC power, but also an efficient and high-power quality interface to AC systems (e.g., grid, motors) [1] - [4], [3] - [6]. In addition, there is the need to study the reliability of multi-pulse LCC in the *Zhundong-Sichuan HVDC project* which was launched in China to better understand the power and investments involved in making multi-pulse LCC reliable (2015,  $\pm 1100$  kV, 10 GW, 2600 km) [6]. Figure 1 is a summary of potential candidates for a multi-pulse AC/DC rectifier for high-power systems.

Manuscript received January 22, 2017; revised June 08, 2017, August 07, 2017 and September 13, 2017; accepted September 25, 2017. This work was supported in part by European Community 7th framework programme (Number: 909880). (Corresponding author: Tao Jin)

D. L. Mon-Nzongo, P. G. Ipoum-Ngome and Tao Jin are with the Electrical Engineering Department of Fuzhou University, Fuzhou, 350116, China (e-mail: monnzongo@fzu.edu.cn; ipoum24@yahoo.fr; jintly@fzu.edu.cn).

J. Song-Manguelle is with ExxonMobil Development, Houston, TX 77060-1905 USA (e-mail: joseph.m.song@exxonmobil.com).

**a) Conventional multi-pulse AC/DC.** This rectifier is the earliest and most widely known technology that is used within HVDC and VFD systems. It is efficient and gives a large amount of power, it is also reliable, and its architecture may allow it to continue to operate even in faulty conditions [5] - [7]. Fig. 1a is a 12-pulse rectifier-based thyristor which is also known as a 12-pulse LCR (load commutated rectifier). It is a current source converter that consists of a 12-pulse transformer (or phase-shifting transformer) and two series-connected 6-pulse rectifiers. The shifting angles ( $\delta_1 = 0$  and  $\delta_2 = 30^\circ$ ) between each secondary winding and the primary winding of the transformer are key elements for obtaining pulsating DC power with reduced voltage ripples and current harmonics at the grid side.

However, the structure of the 12-pulse transformer does not enable the rectifier to operate efficiently in a degraded mode. For example, a severe failure in any part of a transformer may result in a total system shut down if no redundant transformer is installed; additionally, including a redundant transformer will increase the size and cost of the rectifying system.

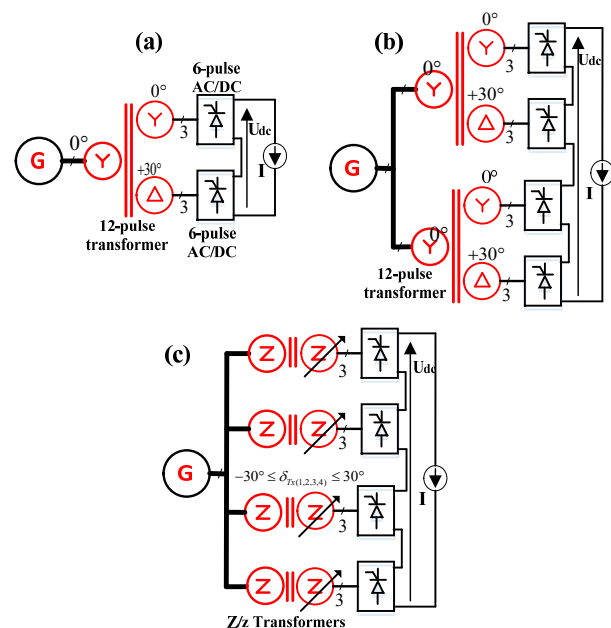


Fig. 1. Topology candidates for high-power AC/DC converters: (a) conventional 12-pulse converter, (b) modern 12-pulse converter, (c) proposed topology.

**b) Modern multi-pulse AC/DC rectifier.** To overcome the issue related to single-thread 12-pulse converters, series, or parallel

connections of two or more 12-pulse converters have been developed in many projects [1,5,6]. Fig. 1b shows an example of a 12-pulse rectifier with two threads or modules (12-pulse transformer and rectifier) connected in series at the DC side. In contrast to the topology shown in Fig. 1a, this setup can continue to operate as a single-module 12-pulse rectifier in the case of failure of one module.

The main drawback of this topology is the poor current harmonic performance at the grid-side, since it always operates as a 12-pulse rectifier in a normal or degraded mode of one module. Therefore, it requires the same filtering devices of the same size as a single-thread 12-pulse rectifier shown in Fig. 1a. The use of filtering devices in high-power systems may increase the risks of electrical resonance with AC systems (e.g., electric network, AC motors).

The topology shown in Fig. 1b can be improved to operate as a 24-pulse rectifier in normal mode if only the two windings at the primary side of the 12-pulse transformers are configured in a zigzag to generate phase shifting angles of  $+7.5^\circ$  and  $-7.5^\circ$ . However, in this configuration, the 24-pulse rectifier can only operate as a 6-pulse rectifier in a degraded mode, since the phase-shifting angle does not correspond to an 18-pulse or 12-pulse operation.

**c) Proposed topology:** Using the same number of 6-pulse rectifiers as shown in Fig. 1b but with four separated three-phase variable phase shifting transformers instead of two 12-pulse transformers, we propose a new topology, as shown in Fig. 1c. The proposed topology operates as a 24-pulse rectifier in its normal mode and, respectively, as an 18-, 12- and 6-pulse rectifier in the case of one, two or three faulty modules in the degraded mode. Compared to the topology of Fig. 1b, this topology can withstand the same amount of power when using the same power rating as its transformers and rectifiers. Moreover, it generates fewer AC components superposed to the DC-side voltage and fewer current harmonic components propagated at the grid side.

In practice, three-phase transformers are easier to manufacture compared to multi-pulse transformers; thus, the proposed topology operating in normal mode with a constant phase-shifting angle can be less expensive than standard topologies. In this paper, the variable three-phase-shifting transformer is called the electronics Z/z transformer, since its phase-shifting angle and voltage ratios are both variable through the electronics interface associated with the tap change of each of the windings. The choice of adding this electronic function to the three-phase transformer will depend on the design objective and the investment involved because the additional electronic function is only activated in a faulty condition and requires additional switches and a control algorithm to operate in a degraded mode.

The traditional topologies of multi-pulse AC/DC converters operating in a degraded mode are described in section II, and the proposed topologies are described in section III.

The new concept, an electronics Z/z transformer is described in section IV. An experimental prototype of an 18 kVA, 1.5 kV, 18-pulse AC/DC converter with the associated control system has been designed and tested to validate the proposed concept.

Simulation and experimental results are discussed in section V.

## II. THE TRADITIONAL TOPOLOGY OF A MULTI-PULSE AC/DC RECTIFIER OPERATING IN A DEGRADED MODE

Fig. 2 is an example of a standard rectifier topology adopted in high-power HVDC or VFD systems [1-5]. It is a 24-pulse rectifier system including a set of phase-shifting three-phase transformers and four series-connected 6-pulse rectifier modules. For this specific configuration, there is a  $15^\circ$  phase-shift between the secondary side voltages of the transformer.

To increase the availability of such system, the input rectifier system should tolerate faults occurring in a partial module (M1 to M4), therefore output DC bypass switches have been inserted in Fig. 2. For the system to operate with failed modules, the voltage phase-shift should be changed from  $15^\circ$  to  $20^\circ$ , then  $30^\circ$  for respectively a healthy system, a degraded 18-pulse with one failed module and a degraded 12-pulse with two failed modules for example. Unfortunately, since the voltage phase-shifting angles are all constant per design, it might become challenging to fulfil the grid side current harmonic requirements such as specified in international standard [17].

From Fig. 2, let's consider  $k_{1x(1,2,3,4)}$  and  $k_{y2(1,2,3,4)}$  as two complementary switches associated to each partial module. If only one module is faulty, then  $k_{1x} = 0$  and  $k_{y2} = 1$ ; the remaining modules can continue to operate but with a reduced power.

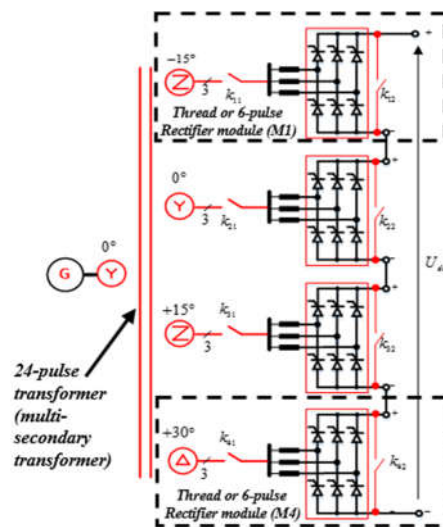


Fig. 2. Traditional 24-pulse rectifier with additional bypass switches

Consequently, per current phasor summation requirement, the system can only operate in 18 or 12 configurations if the phase shift angles of each case are respected ( $\pm 15^\circ$  or  $\pm 20^\circ$ ). This is particularly true in VFD applications where a floating grounding point is used on the DC-side (i.e., the DC-link is not grounded). In such case, the system is only grounded in the primary side of the multi-secondary transformer. As a result, the system can operate safely and can be downgraded (with a reduced power rating) from a 24-pulse rectifier to an 18, 12 or even 6-pulse rectifier.

In HVDC transmission systems with a 24-pulse rectifier, three DC cables are used: positive and negative rails use a

returning DC cable connected at the center point of the system in order to carry more power and also to limit the grounding voltage and voltage stress on the power modules. A failure of a single module on the positive rail, for example, requires bypassing an extra module on the negative rail (with a 50% power reduction) and leads to a 12-pulse rectifier system.

Table I shows all possible faulty modules and switches states for a VFD system to operate in a degraded mode. This table is not applicable to HVDC systems with three-pole cables.

TABLE I: POSSIBLE OPERATING MODES OF A 24-PULSE RECTIFIER IN FAULTY CONDITION OF A PARTIAL 6-PULSE MODULE

$M_1$	$M_2$	$M_3$	$M_4$	$k_{12}$	$k_{22}$	$k_{23}$	$k_{24}$	$S_1$	$S_2$
0	0	0	0	0	0	0	0	24P	24P
0	0	0	1	0	0	0	1	-	18P
0	0	1	0	0	0	1	0	-	18P
0	0	1	1	0	0	1	1	-	12P
0	1	0	0	0	1	0	0	-	18P
0	1	0	1	0	1	0	1	12P	12P
0	1	1	0	0	1	1	0	-	12P
0	1	1	1	0	1	1	1	6P	6P
1	0	0	0	1	0	0	0	-	18P
1	0	0	1	1	0	0	1	-	12P
1	0	1	0	1	0	1	0	12P	12P
1	0	1	1	1	0	1	1	6P	6P
1	1	0	0	1	1	0	0	-	12P
1	1	0	1	1	1	0	1	6P	6P
1	1	1	0	1	1	1	0	6P	6P
1	1	1	1	1	1	1	1	-	-

Let's consider the following notation  $M_{x(1,2,3,4)} = 0$  corresponds to a healthy module, while  $M_{x(1,2,3,4)} = 1$  is for a faulty module. In general, if  $n$  is the number of modules, the system will generate  $p$ -pulse on the dc side (with  $p = 6n$ ), with the secondary side voltages of the transformer regularly shifted by  $60/n$  degrees. Consequently,  $2^n - 2$  corresponds to 14 possible failures. In the  $S_i$  solution (see Table I), using a standard 24-pulse rectifier with additional bypass switches as shown in Fig 2, there are six possibilities to operate in a degraded mode: two modes as 12-pulse rectifier (12P) and four modes as 6-pulse rectifier (6P). During each mode, the pulsating DC power transferred to the dc link corresponds respectively, to a half and a quarter of the total power under normal operation (no faulty module). Conversely, the topology shown in Fig. 2 is in opposition to optimal an operation in a degraded mode, since it leaves 8 modes among 14, where a 24-pulse rectifier can no longer operate in analytical conditions for current harmonic cancellation [4].

Therefore, a solution based on a Z/z transformer has been proposed. The resulting number of pulses in degraded conditions are shown in table II (see S2 column). With the proposed approach, all 14 possibilities can lead to a system operating in a degraded mode with a substantially high number of pulse as indicated in Table II. Among them, there are 04 modes corresponding to 18-pulse (18P), 06 modes to 12-pulse (12P) and 04 modes to 6-pulse (6P) rectifiers. Thus, the same installation of a 24-pulse rectifier can operate as three different number of pulse in a degraded mode, without adding any new full three-phase transformer to the system. However, a

supplementary circuitry will be required as discussed in the next section.

### III. PROPOSED TOPOLOGY: Z/Z TRANSFORMER

Because of the significant investment involved in high-power HVDC systems such as those listed in [6], ongoing HVDC projects in China are intensifying research regarding fault-tolerance techniques in AC/DC and DC/AC systems. Recent investigations in this area are mainly focused on the power conversion stage with IGBTs or IGCTs, and their control and modulation strategies, [9]-[11]. This section describes an approach focused on increasing the availability of a multi-winding transformer and multi-pulse rectifier system for HVDC transmission systems, by using separated three-phase transformers with adjustable phase-shift angles of their voltage, instead of a single multi-secondary transformer with constant angle per design. Obviously, the proposed solution is also applicable to large VFDs with tight requirements on grid side current THD.

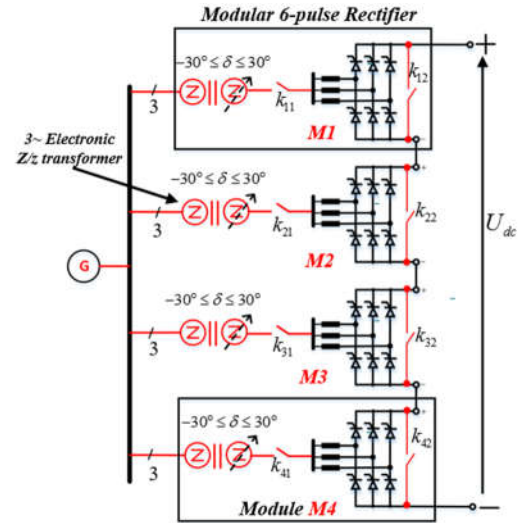


Fig. 3. Proposed topology for a 24-pulse rectifier-based four Z/z transformers, that provides variable-shifting angles and turn ratios.

Figure 3 shows the simplified single-line diagram of the investigated topology for a specific case of a 24-pulse AC/DC converter. The configuration can also be used on the inverter side of a load-commutated-inverter drive or on the receiving end of an HVDC system with minor modifications and for higher number of pulses. The architecture is based on the series-connected 6-pulse rectifier modules supplied by electronic Z/z transformers that enable possible operation in a degraded mode by providing the corresponding phase-shifting angles.

The topology uses four separated three-phase transformers, where the primary and secondary windings are initially configured in a zigzag formation and includes tap-changing windings that can be adjusted through power switches configured as described in the next section in order to obtain adjustable phase-shifting angles and voltage ratios. The system can also be used with traditional tap-changing switches. If one module is faulty, the remaining transformer's phase-shifting angles will be adjusted to generate the corresponding angles and

voltage ratios to operate as an 18-pulse rectifier and to maintain the adjusted amount of power. These angles are, respectively  $-20^\circ$ ,  $0$  and  $+20^\circ$ . The voltage ratio can be kept equal to  $1/4$  of that in the normal mode or can be increased to  $1/3$  in order to compensate for the diminution of power due to the faulty module, which is bypassed.

However, it is challenging to have an exact voltage boost to compensate for the loss of power; therefore, a slight decrease in the overall power is expected. Normally, the system should be designed with a sufficient voltage margin such that during the transformer reconfiguration the transformer voltage is slightly boosted to compensate for the possible voltage loss due to the bypass of the faulty module.

As explained in section II, solution  $S_2$  shown in Table I, indicates all possible modes that can be obtained. They are dependent on the number of faulty six-pulse modules. Unfortunately, increasing the number of components will reduce the system reliability, and consequently, they should be included in the plant maintenance plan. However, this solution can achieve greater system availability with grid-side current THD within acceptable margins such as the ones specified in IEEE 519 [17] as well as reduced loss of power when at least one module is faulted and bypassed.

#### IV. AN IMPLEMENTATION METHOD OF A THREE-PHASE ELECTRONICS Z/Z TRANSFORMER

##### A. General Principle

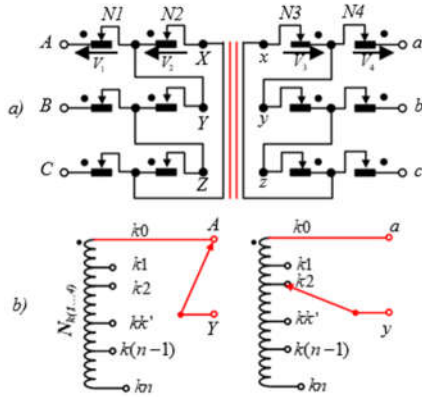


Fig. 4. General principle of a three-phase electronic Z/z transformer: (a) Transformer connected in Z/z, (b) taps change variation principle.

Figure 4 shows the configuration of the windings and the step variation mechanism of an electronic Z/z transformer. The primary and secondary windings consist of  $N_{k(1,2,3,4)}$  windings.  $N_1$  and  $N_2$  are located on the primary side, while  $N_3$  and  $N_4$  are those located on the secondary side, as shown in Fig. 4a. Initially, the primary and secondary windings are in a zigzag connection (Z/z). By knowing that the Z/z connection is the combination of the wye and delta connections, it is possible to obtain one of them by properly selecting the tap level of each winding. For example, if  $N_2 = 0$  and  $N_3 = 0$  the transformer has a wye-wye (Y/y -  $0^\circ$ ) formation. Similarly, if  $N_2 = 0$  and  $N_4 = 0$  the transformer is configured in wye-delta (Y/d -  $30^\circ$ ). Thus, the Z/z transformer represented in Fig. 4a can be configured to adjust predefined phase shift angles.

Each winding  $N_{k(1,2,3,4)}$  in Fig. 4a consists of  $kn$  tapping coils, as shown in Fig. 4b. The windings variation principle is to step the cursor  $k'$  from  $kn$  to  $k0$  or in the reverse direction. When the tap cursor of windings  $N_1 - N_2$  or  $N_3 - N_4$  is between  $k0 \leq k' \leq kn$ , the windings are connected in a zig-zag formation. They are configured in delta or wye connections when the cursor is at the same position as  $k0$  or  $kn$ . The discrete change of the phase-shifting angle and the winding turn ratio is adjusted to define the correct value of  $N_1$  to  $N_4$  in a degraded mode and are pre-designed as described in [4].

##### B. Summarized voltage phasor analysis for the tap change windings design

Figure 5 shows possible configurations of a Z/z transformer. To design each tap winding, consider  $N_2 = 0$  and the phase-shifting angle defined as  $0 < \delta < 30^\circ$ . For this case, the Z/z transformer which was shown in Fig. 4a becomes equivalent to the structure represented in Fig. 5a-1 and its equivalent phasor diagram is presented in Fig. 5a-2. In the same way when  $N_1 = 0$  and the phase-shifting angle defined as  $30^\circ < \delta < 0$ , the Z/z transformer of Fig. 4a becomes equivalent to Fig. 5b-1 and its voltage phasor diagram is shown in Fig. 5b-2. Applying basic trigonometric formulas to these two phasor diagrams, for respectively the triangle  $o S_1 S_3$  and  $S_1 S_2 S_3$  then  $o S_1 o_1$  and  $S_1 S_2 S_3$  respectively as shown in Fig. 5a-2 and Fig. 5b-2, we obtain Eq. (1) and Eq. (2) given below. It is these equations which are used to preset the number of turns of each tap winding corresponding to a specific operating mode.

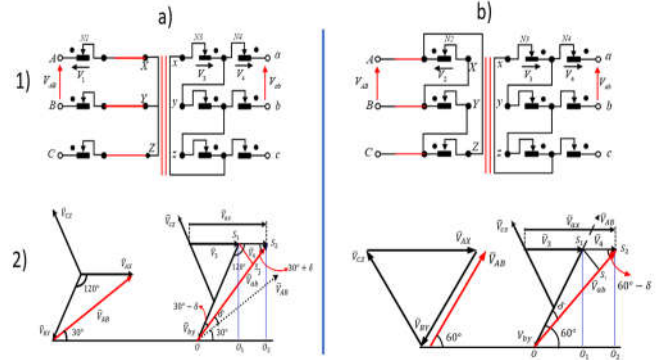


Fig. 5. Different configuration of a Z/z transformer. a-1) Y/z transformer connection; a-2) phasor diagram. b-1) D/z transformer connection; b-2) phasor diagram.

$$\begin{cases} \frac{N_4}{N_3 + N_4} = \frac{V_4}{V_{ax}} = \frac{\sin(30^\circ - \delta)}{\sin(30^\circ + \delta)} \\ \frac{N_1}{N_3 + N_4} = \frac{V_{Ax}}{V_{ax}} = \frac{1}{2 \sin(30^\circ + \delta)} \frac{V_{AB}}{V_{ab}} \end{cases} \quad (1)$$

$$\begin{cases} \frac{N_4}{N_3 + N_4} = \frac{V_4}{V_{ax}} = \frac{\sin(\delta)}{\sin(60^\circ - \delta)} \\ \frac{N_2}{N_3 + N_4} = \frac{V_{Ax}}{V_{ax}} = \frac{\sqrt{3}}{2 \sin(60^\circ - \delta)} \frac{V_{AB}}{V_{ab}} \end{cases} \quad (2)$$

In practice, it is very difficult to obtain more than two faulty rectifier modules at the same time. Therefore, the realistic case consists to design a Z/z transformer that can operate from 24-

pulse to 18-pulse rectifier (with two modes only). Thus, the phase-shifting angles are respectively  $0, \pm 15^\circ, 30^\circ$  for a normal mode operation, and  $0, \pm 20^\circ$  in a degraded mode operation. When the number of operating mode is known, the number of tap windings is defined (two taps for this case) and the topology of the power switches associated to these tap windings is also derived as explained in next section.

### C. Implementation for a 24-pulse rectifier

An example for the implementation of Z/z transformers for a 24-pulse rectifier with the original phase-shifting angles of  $0, \pm 15^\circ$  and  $30^\circ$  is shown in Fig. 6. These angles should be readjusted to  $0, \pm 20^\circ$  in a faulty condition. Their primary windings are configured in Y-grounded with bidirectional power switches associated to the secondary windings to achieve the discrete variation of the transformer's phase shift angle.

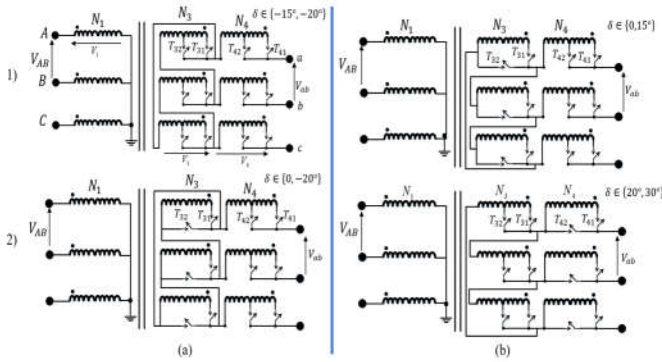


Fig. 6. Detailed windings and power switches configuration a) positive and b) negative phase-shift.

Fig. 6a shows the detailed connections of the transformer's windings for generating negative phase-shifting angles. In Fig. 6a-1, the first set of windings generates the phase-shifting angle of  $15^\circ$  when the power switches  $T_{32}$  and  $T_{41}$  are closed and  $T_{31}$  and  $T_{42}$  are open. Otherwise it produces a phase shift of  $20^\circ$ . The transformer configured as shown in Fig. 6a-2 generates  $20^\circ$  when  $T_{31}$  and  $T_{42}$  are closed and  $T_{32}$  and  $T_{41}$  are opened. Otherwise, it produces a phase shift of  $0^\circ$ . Fig. 6b shows the detailed connections of three-phase transformer's windings for generating positive phase-shifting angles. In Fig. 6b-1, a  $+15^\circ$  phase-shift is obtained when  $T_{31}$  and  $T_{42}$  are closed while  $T_{32}$  and  $T_{41}$  are opened.  $+20^\circ$  is obtained from the transformer shown in Fig. 6b-2 when  $T_{32}$ ,  $T_{41}$  are closed while  $T_{31}$ ,  $T_{42}$  are opened. Otherwise, these transformers will generate the phase shift angle of  $0^\circ$  (Fig. 6b-1) and  $+30^\circ$  (Fig. 6b-2).

$$\begin{cases} V_1 = \frac{4}{\sqrt{3}} V_{ab} = \frac{V_{AB}}{\sqrt{3}} \\ V_3 = 2 \sin(30^\circ + |\delta|) \left( 1 - \frac{\sin(30^\circ - |\delta|)}{\sin(30^\circ + |\delta|)} \right) \frac{V_{ab}}{\sqrt{3}} \\ V_4 = 2 \sin(30^\circ - |\delta|) \frac{V_{ab}}{\sqrt{3}} \end{cases} \quad (3)$$

The four transformers configured as shown in Fig. 6 have twelve power switches per transformer. If a fault occurs in only one of the rectifier modules of the 24-pulse rectifier, the system is downgraded to an 18-pulse rectifier by adjusting the voltages across  $N_3$  and  $N_4$ . The desired voltage and phase-shifting angle are pre-designed as described previously and the final equations to obtain the voltage across each tap winding are given in Eq. (3).

The additional power losses due to the power switches have been estimated to 0.15% of the global DC power that can be generated by each six-pulse rectifier module for a 10 MW VFD system. We emphasize that, the losses calculation was based on the IGBT FZ1200R17HE4P of Infineon with the rated power of 2 MW and dynamic characteristics described in [21]. We have also assumed that the conduction losses of the IGBT antiparallel diode and switching losses are negligible since in this utilization the power switches do not continuously switch in steady state as it would be in VFD application. Only the on-state conduction losses were considered. Thus, for the implementation of an input transformer of a 24-pulse rectifier configured as shown in Fig. 6, the power losses will be approximately 15 kW per transformer.

### D. Control architecture for a 24-pulse rectifier system

Figure 7 shows a high-level overview of the system control architecture of a multi-pulse LCI, with p-pulse on the rectifier side and q-pulse on the inverter side. A similar configuration can be adopted for HVDC transmission system as shown in Fig. 8. Each power conversion unit (Rectifier or sending-end, inverter or receiving end) has a dedicated slave controller synchronized through the grid-side or motor-side voltage, and they are supervised by two independent master controllers. The transformer has its own controller integrating protection functions. In VFD applications these functionalities can be integrated to one physical controller, with some of the transformer protective functions handled by industrial protective relays [16], [18-19].

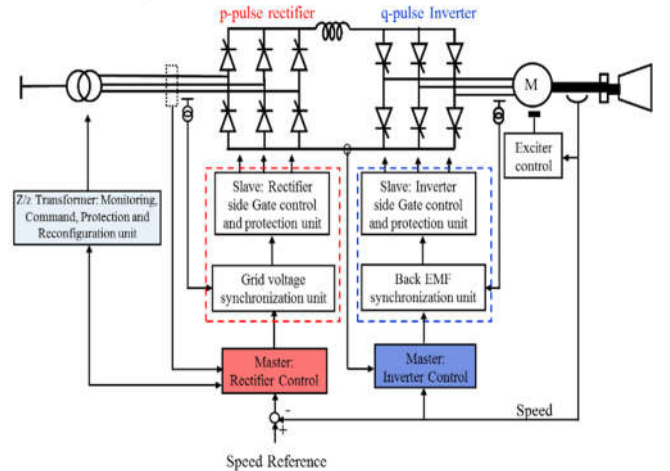


Fig. 7: High-level overview of the control system of a multi-pulse LCI VFD

Figure 8 shows a detail functional architecture of the rectifier or sending-end power converter unit. Each rectifier module has a local slave controller for its gating, protective functions and grid synchronization. There is a master controller for the startup and shutdown sequential control, a closed-loop controller for

speed or torque (VFD application) as well as the control of DC-link current (e.g. internal VFD DC-link or transmission current control). And finally, there is a Z/z transformer command module with monitoring, gate drivers level and power system protective functions with relaying per IEEE C37.2 standard [16]. This module is taking of the transformer reconfiguration through the power switches.

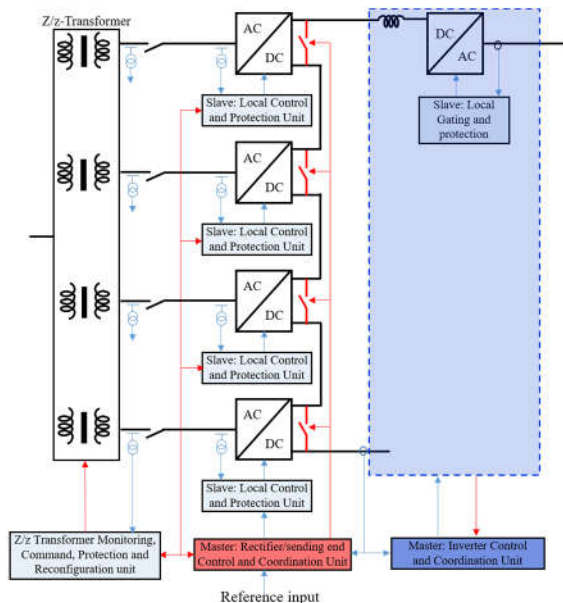


Fig. 8: Control architecture of input rectifier with a Z/z-Transformer.

In general, the control strategy for the local controller used in standard VFDs and HVDC systems is often based on linear controllers (PI regulators with possible decoupling network and anti-windup strategies), the synchronization unit is a phase-locked-loop (PLL) which is based on a voltage controlled oscillator in series with a low-pass filter for the control of the angular frequency of the grid voltage or motor-side back EMF (in VFD systems). Initial implementation for such functions can be found in most of commercial time-domain transient simulator software in electrical engineering [22-24]. For example, a model for implementing a single pole HVDC system including all functions as represented in Fig. 8 is available in the library models of [22]. Similar master/slave controller can be found in [5].

### E. Notes on industrial system implementation

For industrial systems, there is no need for a special fault detection circuit. Instead, existing protection features for such systems can be used. These features include the following [16]: i) transformer monitoring and protection through industrial protective relays, such as instantaneous overcurrent (50), AC time overcurrent (51), as well as differential protection relays (87); ii) sending-end converter overcurrent protection (instantaneous and AC time overcurrent, 50/51); iii) under-voltage protection (27) and under-frequency protection (81U); iv) overall converter monitoring system resulting from the gate drivers; and v) earth-fault protection in the power stages.

In addition, because of the power level and voltage rating of large power systems (e.g., HVDC and large VFDs), it is beneficial to clearly state that the system should not be

reconfigured online. All the aforementioned fast protective functions should act normally to protect the integrity of the system, including opening the main breaker, which may lead to a partial system shutdown if required.

Usually, the reconfiguration of the system should be decided by the plant electrical team after a trip and also as a result of a quick root cause failure assessment. Once it has been confirmed that the fault is only impacting a rectifier module, the electrical team can proceed with system reconfiguration. Such an approach is recommended in industrial applications in order to avoid consequential failures of other parts of the power system that may result from the transient behavior of faulted power equipment.

A control algorithm that takes into account a pre-identified system reconfiguration and that is based on Table I will be developed and executed through the HMI control panel. A reconfiguration guide should be provided to the electrical team in order to easily resume the system operation in a degraded mode. Specifically, for HVDC applications, the management of the failure of one module on the positive or negative pole should be done during the design stage as follows:

i) A system should be designed with a 25% voltage margin: in the design stage, the overall system can be designed to output 125% of the needed power in order to achieve a global 25% power redundancy. In that case, bypassing a healthy rectifier module will reconfigure the rectifier side from a 24- to a 12-pulse system; this will then achieve 75% of the nominal power available instead of 50% if the system is designed without a voltage margin.

ii) A system designed with a 25% voltage reserve and a 25% current margin: more power might be achieved if the design team decides to select the overall current transmission with up to a 25% current margin combined with a 25% voltage reserve. In that case, once the system is reconfigured from 24-pulse to a 12-pulse degraded mode, the current reference is ramped to 125% of the nominal transmission power; therefore, the achievable power can reach approximately 93.75% of its nominal power. However, this type of design will increase transmission losses and produce a high magnitude of low-order harmonics. The design team should take such considerations into account, as well as conduct a trade-off study for selecting the setup of the final design specifications.

## V. SIMULATION AND EXPERIMENTAL ANALYSIS

### A. Simulation set-up and results

For validation, simulation models of a 24-pulse rectifier system, as shown in Fig. 2 and Fig. 3, have been developed with the software Simpowersystems of MATLAB/Simulink. The model of the transformers was implemented using basic single-phase transformers with seven tap windings per device to the secondary side for demonstration purposes only. Bidirectional power switches are used. The fault detection circuit was implemented as described in [18]. The control logic of switches associated to the tap windings of each transformer was developed to include all operating mode as described in Table I. The turn and voltage ratios for each mode were pre-calculated

as described in Eq. (1) and Eq. (2). These values were used to configure the primary side of the transformers and then identify the desired number of windings at the secondary side. The parameters of the simulation are shown in Table II, and the results are shown in Figure 9.

TABLE II: PARAMETERS

Parameters	Values in simulation	Values in experiment
Supply voltage	1440 V	380 V
Supply frequency	50 Hz	50 Hz
Line reactor	1 mH	2.5 mH
Transformers	150 kW	9 × 2 kVA/ 3 devices by cabinet
Voltage ratio	Variable	Constant : M=1/3
Turn ratio	Variable	0.227 and 1.96
Rectifier	<b>24-pulse</b>	<b>18-pulse (degraded from 24-pulse)</b> 3 × 500 V 18 kW
Load	Current source (50 A)	3 kW and 6 kW RL load \ 100 Ω and 40 Ω , 50 mH)
Thyristor firing angle	$\alpha = 30^\circ$	$\alpha = 0$

Figs. 9a, 9b and 9c were obtained when validating the proposed electronics Z/z transformer. Two open circuit faults on partial modules were simulated to observe the performances of the entire system in degraded modes. Fig. 9a, shows that before the instant 0.06 s, all transformers are operating in normal condition. The phase-shifting angle between two

consecutive line-to-line voltages is  $15^\circ$  as shown in Fig. 9b, and the voltage ratio is  $\frac{V_{ab}}{V_{AB}} = \frac{1}{4}$ . After 0.06s, the first preprogrammed fault was detected on M4 and then isolated from the rest of the system, including its transformer. Therefore, the remaining healthy transformers are reconfigured to produce the phase shifting angles of  $20^\circ \leftrightarrow 0 \leftrightarrow +20^\circ$  (Fig. 9b) and voltage ratio  $\frac{V_{ab}}{V_{AB}} = \frac{1}{3}$  (Fig. 9c). A similar scenario occurs at time 0.12 s, where a second preprogrammed fault was detected on modules M3 and M4. As shown in Fig. 9b and Fig. 9c, the remaining transformers are reconfigured so that  $30^\circ \leftrightarrow 0$  is the shifting angle between them. This configuration is required for a 12-pulse rectifier.

Because electronic Z/z transformers can change their phase-shifting angles and voltage ratio, the 24-pulse rectifier system can then operate optimally. It configures itself to the nearest pulse number based on the number of faulty modules (Fig. 9d, 9e and 9f). Fig. 9d shows the total pulsed DC voltage at the DC side of the 24-pulse rectifier proposed in Fig. 3. This figure illustrates that, the DC voltage dynamically changes the number of pulses from a normal mode of operation (24-pulse) to any degraded mode corresponding to any number of faulty modules. For example, during the time 0.04 to 0.08 s, in Fig. 9d the rectifier is operating as an 18-pulse rectifier because the number of remaining modules is  $n = 3$ . Moreover, during the instants 0.08 to 0.12 s and 0.12 to 0.16 s, the output DC voltage of the rectifier respectively produces 12 and 6 pulses since two and three faulty modules were detected.

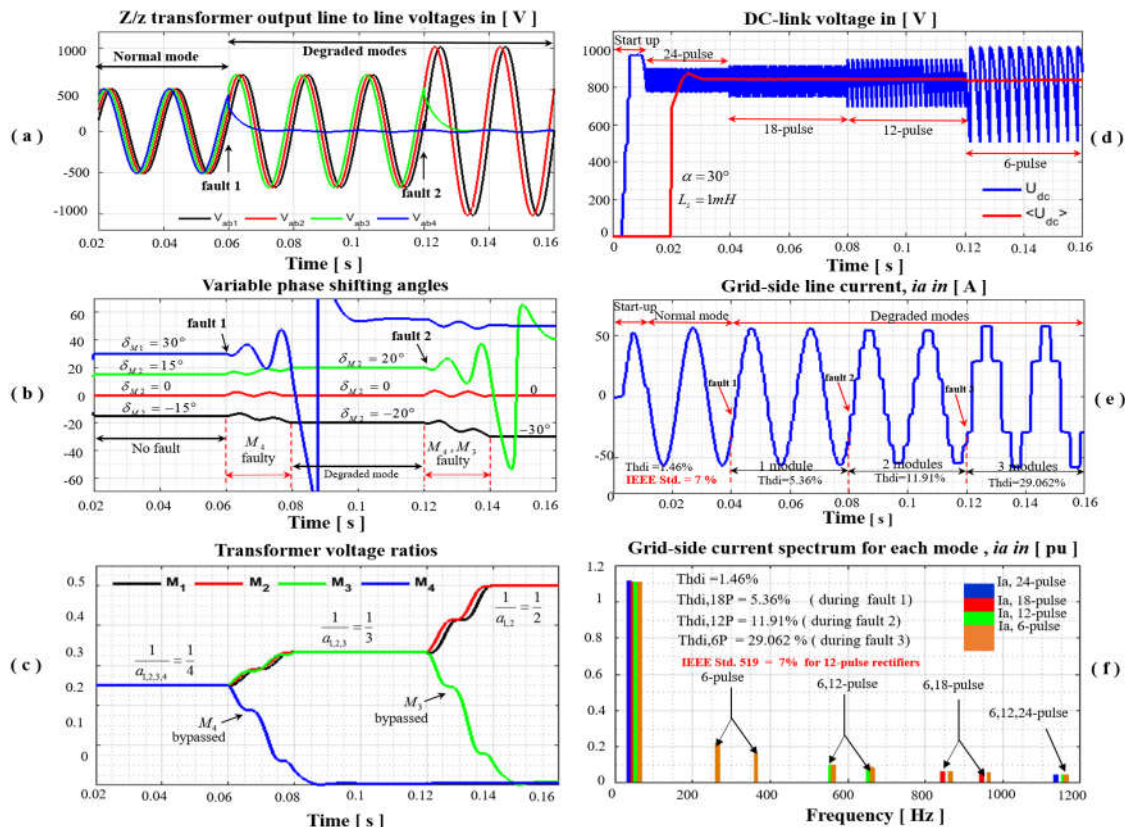


Fig. 9. Simulation results of a 24-pulse rectifier based electronic Z/z transformers in normal and degraded mode. (a) Line-to-line voltage of transformers, (b) phase shifting angles, (c) voltage ratios. (d) total DC-link voltage, (e) total grid-side current, (f) propagated current harmonic spectrum of each mode at the grid-side.

Fig. 9e shows the input AC current profile at the primary side of all transformers (for only one phase). This is a well-known grid-side current profile due to rectifier-systems-based thyristors or diodes [4]. But in this case, the frequency of the harmonics is adjustable. When neglecting inter-harmonics, the frequency  $f_{h,n} = |6n \pm 1|f_1$  of the current harmonic changes as a function of the number of remaining modules  $n$ . Moreover,  $h$  is the harmonic rank,  $h=0, 1, 2$ , etc. If only one module is faulty, then  $n = 3$ . Thus, the frequency of the current harmonics is  $f_{h,3} = |18 \pm 1|f_1$ . For  $h = 1$  and  $f_1 = 50$  Hz, we obtain the frequencies of negative and positive sequence harmonics equal to 850 Hz and 950 Hz, as shown in Fig. 9f. This also shows the total harmonic distortion  $THD_i$  in the normal and degraded modes. These values can be compared to the one recommended by IEEE standard 519 for a 12-pulse rectifier.

In summary, the rectifier system remains in operation in a degraded mode with a reduced harmonic performance compared in the normal mode. However, the main benefit of using this approach is its capabilities in faulty conditions, especially in the 18-pulse mode, because it allows the system to continue delivering power with better quality while awaiting technical solutions for its maintenance.

### B. Performance comparison between the standard topology (Fig. 2) and proposed topology (Fig. 3)

This sub-section compares the standard and proposed topologies. The electronics Z/z transformers are set so that they do not boost the voltages in faulty conditions. In this case, their voltage ratio does not change as in a conventional 24-pulse transformer. Figure 10 shows the results of the comparison in the time domain (Fig. 10a and 10b) and in the frequency domain (Fig. 10c).

In a previous discussion, it was demonstrated that the 24-pulse rectifier-based topology in Fig. 3 can optimally operate as an 18-, 12-, or 6-pulse rectifier in a degraded mode. However, this is not possible with the traditional topology (Fig. 2). The difference is illustrated through Figs. 10a and 10b. There, it can be seen that in normal mode (i.e., M1 to M4 are healthy), the DC-link voltages and AC current waveforms are the same in the steady state for both topologies and operate as a 24-pulse rectifier. However, when one or two modules are faulty, the traditional topology (Fig. 2) can no longer operate as an 18- or 12-pulse rectifier. This can be verified by counting the number of pulses of the variable denoted by  $U_{dc}$  (Fig. 2) from 0.04 s to 0.06 s and from 0.06 s to 0.08 s (one cycle of the fundamental current). The results show six pulses per cycle for the black color curve. These results are confirmed in the frequency domain (Fig. 10c), where the amplitudes of the relevant current harmonic waveforms, denoted by  $I_h$  (Fig. 2) have their peak values at 250 Hz even when only one module is faulty. Taking as an example only the case where the module M4 is faulty, it can be seen that between the frequency interval of 250 and 950 Hz, the amplitude waveform of the current harmonics is the same as in the case where M4, M3, and M2 (three modules) are faulty. Then, its trajectory changes between 950 Hz to 1250 Hz (see  $I_h$  of Fig. 2 in Fig. 10c for only an M4 faulty).

In a degraded mode, it can be stated that, at low frequencies (below 950 Hz), a traditional topology that is based on a 24-

pulse rectifier operates as a 6-pulse rectifier with increased current distortions compared to those obtained in the same conditions when using the proposed topology (see  $THD_i$  in Fig. 10c). However, when three modules are faulty, the two topologies behave similarly. The total harmonic distortion is around 24.5%, which is above the recommended value for 6-pulse rectifiers. Thus, if no filtering solutions are available, the system may be shut down for both topologies.

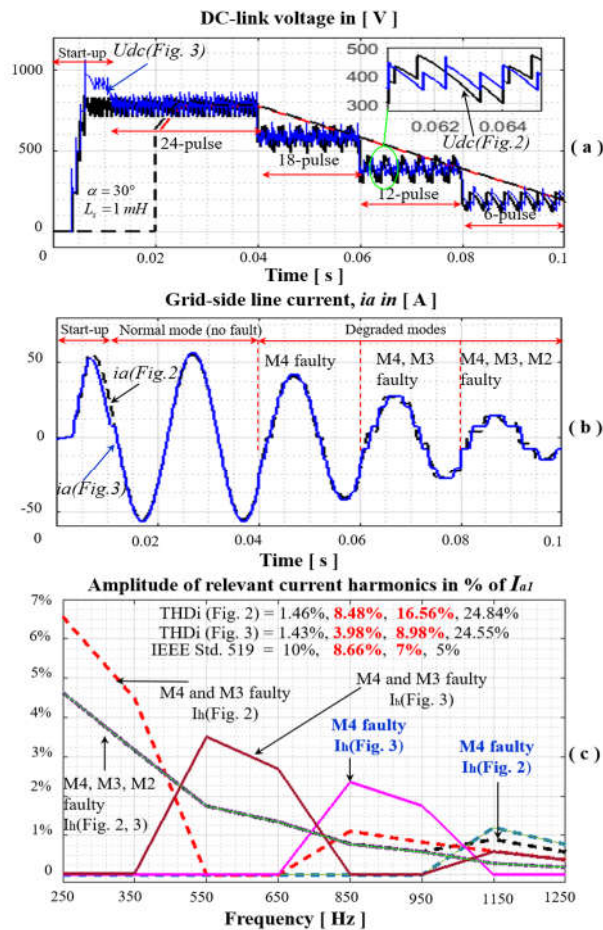


Fig. 10. Simulation results of 24-pulse rectifier based traditional (Fig. 2) and proposed (Fig. 3) topologies. (a) DC-link voltage, (b) grid-side current in time-domain, (c) relevant current harmonic amplitudes in frequency domain. The amplitude of the fundamental current is  $I_1 = 56.71$  A (base value).

### C. Experimental set-up and results

For the experimental validation, the simulated system has been reduced as it follows: i) the system implemented is an 18-pulse rectifier degraded from 24-pulse with a reduced power of 18 kVA. This power is shared between three cabinets of 6 kVA, 18-pulse rectifiers connected in series; ii) per cabinet, three Z/z transformers are used to generate  $0, \pm 20^\circ$  or  $0, 30^\circ$ , as phase-shifting angles respectively in a normal or degraded mode; iii) electromechanical contactors acting as power switches are considered. Thus, gate driver circuits are not needed, including their extra power supplies when using electronics switches such as IGBTs or GTOs; 4i) only the results of one cabinet are discussed in this subsection.

Figure 11 shows the detailed power circuit of cabinet 1 with the photo of the system that was tested to validate our study

(cabinet 1 only). It represents a part of the HVDC and VFD experiment test-bench that is still under development. The control system is based on Simulink real-time, where the host PC includes Simulink software which is used to develop the control algorithm and to generate and download the executable

files for the target PC through TCP/IP. The target PC is an industrial PC-based National Instrument boards PCI-6229, which interfaces the power stage with the control software. For comparison with the simulations, experimental parameters are also shown in Table II, and the results are shown in Fig. 12.

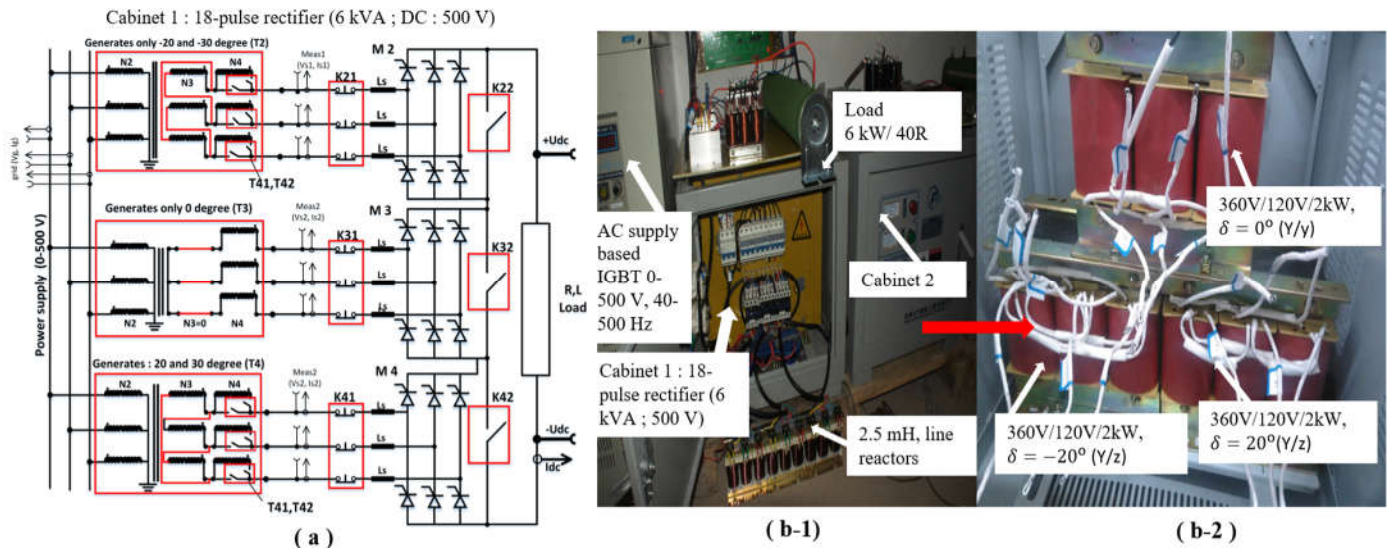


Fig. 11. Simplified laboratory prototype. (a) the detailed power circuit of cabinet 1, (b) photo of cabinet 1 under test with the detailed view of the three-phase Z/z transformers.

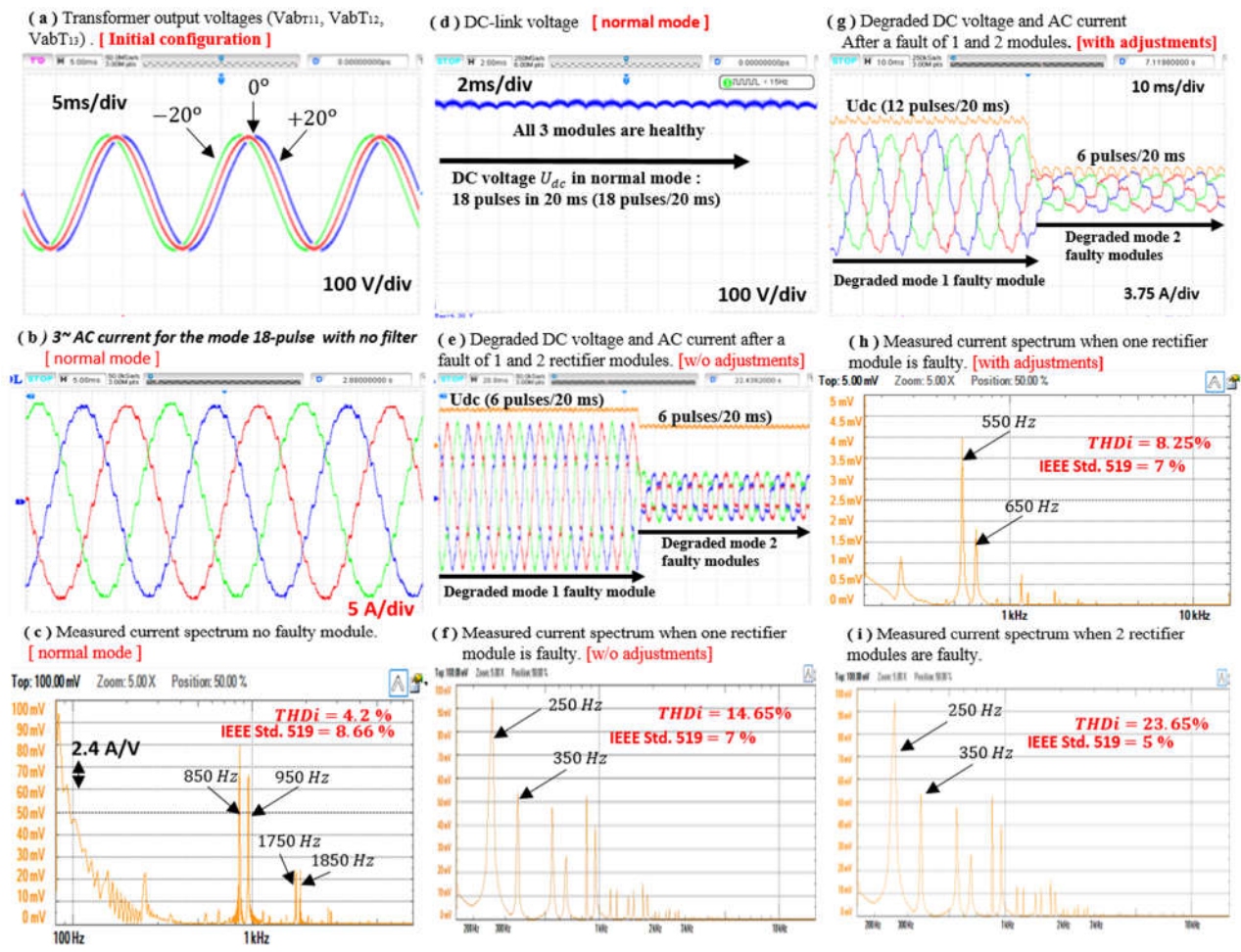


Fig. 12. Experimental results of an 18-pulse rectifier degraded from a 24-pulse rectifier. The normal mode is when the 3 rectifier modules are healthy. The degraded mode is when any of the modules are faulty.

Fig. 12a, shows the measured line-to-line voltage at the secondary side of each partial transformer (see these transformers in Fig. 11b). The objective was to verify whether the phase-shifting angle between transformers corresponds to  $20^\circ$ ; this value represents the selected phase shifting angles for an 18-pulse rectifier operating in normal mode. The results effectively match with the predicted values when neglecting the error of  $0.02^\circ$ .

The experimental results of the 18-pulse rectifier system of cabinet 1 were successful when operating in the normal mode, as shown in Figs. 12b, 12c, and 12d. These values correspond to those obtained from the simulation results when considering an 18-pulse rectifier as the normal mode. The relevant harmonics near the fundamental are exactly at 850 Hz and 950 Hz, as shown in Fig. 12c. The total harmonic distortion is 4.2%, which is slightly above the predicted value shown in Fig. 10c.

In degraded modes, satisfactory results, shown from Figs. 12e to 12i were also obtained. Faulty modules were tested using an open circuit. Two faulty scenarios were pre-programmed in real-time. Fig. 12e shows the results of the first scenario where the designed 18-pulse rectifier operates with two modules, but behaves as a 6-pulse rectifier in terms of the number of pulses over a cycle of the fundamental. After approximately 2 s, the second fault scenario occurs, corresponding to 02 faulty modules, which leads the rectifier to operate with only one module because the phase-shifting angles of the healthy rectifier modules were not adjusted. The dominant current harmonic components in both cases are located at 250 and 350 Hz in degraded modes, as shown in Figs. 12f and 12i. At this point, the total harmonic distortion increased significantly. It was 4.2% in the normal mode and suddenly increased to 14.65 % and then 23.65% for each faulty case (see Figs. 12f and 12i). Those values are above the values specified in the IEEE 519 standard [17].

In Fig. 12g and 12h the results are improved when the phase-shifting angles of healthy transformers are adjusted to  $\delta \in \{0, 30^\circ\}$  for the case with two healthy modules. Furthermore, cancellation of the current harmonics occurs. Now, the relevant low order harmonics are located at 550 and 650 Hz (Fig. 12h) instead of 250 and 350 Hz, as in Fig. 12f, and the total harmonic distortion is improved from 14.65% to 8.25%.

## VI. CONCLUSION

This paper proposed an improved topology of a multi-pulse AC/DC rectifier system to enable a degraded mode operation of VFD and HVDC systems with a faulty transformer or rectifier module but with acceptable grid side current distortion. The analyzed system is based on a 24-pulse rectifier system with four separated three-phase transformers, which are called electronic Z/z transformers, since their phase shifting angles and voltage ratios are reconfigurable through electronic command. The proposed configuration improves the conventional structure of a 24-pulse rectifier system, introducing the ability to adjust and improve the grid side current distortion in a degraded mode.

The principle and an implementation method of the proposed electronics Z/z transformer has been discussed. Moreover, the

integration of the Z/z transformer command unit within the control architecture for VFD and HVDC systems has been presented. Finally, a reduced scale laboratory experimental set-up rated 18 kVA, 1.5 kV and 18-pulse converter has been built and tested to confirm the accuracy of the investigations.

In future, the effects of the additional switches on the dynamic performances of the AC/DC rectifier system will be investigated.

## ACKNOWLEDGMENT

The authors would like to thank the reviewers for their professional contribution and helpful suggestions.

## REFERENCES

- [1] S. Kouro, J. Rodriguez; B. Wu, S. Bernet; M. Perez, "Powering the future of industry": High-Power adjustable speed drive topologies," IEEE Trans. Ind. Appl., Magazine, no. 4, pp. 26-39, July/August 2012.
- [2] H. Abu-Rub, M. Malinowski, K. Al-Haddad, Power Electronics for Renewable Energy Systems, Transportation and Industrial Applications, 1st ed., ser. 1, IEEE Press-Wiley, 2014, UK, vol. 1, ch. 1, pp. 1-26.
- [3] P. Wikstrom, L. A. Terens and H. Kobi, "Reliability, availability and maintainability of high-power variable-speed drive systems", IEEE Trans. Ind. Appl., vol. 36, no. 1, pp. 231-241, Jan./Feb. 2000.
- [4] B. Wu, High-Power Converters and AC Drives, 1st ed., IEEE Press-Wiley, 2006, USA, Part. II, pp. 37-92.
- [5] J. Song-Manguelle, M. H. Todorovic, R. K. Gupta, D. Zhang, S. Chi, L. J. Garcs, R. Datta, and R. Lai, "A modular stacked dc transmission and distribution system for long distance subsea applications," IEEE Trans. Ind. Appl., vol. 50, pp. 3512-3524, Sept 2014.
- [6] J. Cao, J. Y. Cai "HVDC in China," in EPRI 2013. [Online]. Available: [http://dsius.com/cet/HVDCinChina\\_EPRI2013\\_HVDC.pdf](http://dsius.com/cet/HVDCinChina_EPRI2013_HVDC.pdf)
- [7] E. Cengelci, P. N. Enjeti, and J. W. Gray, "A new modular motor-modular inverter concept for medium-voltage adjustable-speed-drive systems," IEEE Trans. Ind. Appl., vol. 36, no. 3, pp. 786-796, May/Jun. 2000.
- [8] T. Geyer and S. Schroeder, "Reliability considerations and fault handling strategies for multi-MW modular drive systems", IEEE Trans. Ind. Appl., vol. 46, no. 6, pp. 2442-2451, 2010.
- [9] B. Mirafzal, "Survey of fault-tolerance techniques for three-phase voltage source inverters", IEEE Trans. Ind. Electron., vol. 61, no. 10, pp. 5192-5202, 2014.
- [10] A. B. Abdelghani, H. B. Abdelghani, F. Richardeau, J. Blaquiere, Franck Mosser, I. Slama-Belkhdja, "Versatile three-level FC-NPC converter with high fault-tolerance capabilities: switch fault detection and isolation and safe postfault operation", IEEE Trans. Ind. Electron., vol. 64, pp. 6453-6464, 2017, ISSN 0278-0046.
- [11] Y. Song and B. Wang, "Survey on reliability of power electronic systems", IEEE Trans. Power Electron., vol. 28, no. 1, pp. 591-603, Jan. 2013.
- [12] D. Kastha and B. K. Bose, "Investigation of fault modes of voltage-fed inverter system for induction motor drive", IEEE Trans. Ind. Appl., vol. 30, no. 4, pp. 1028-1038, Jul./Aug. 1994.
- [13] M. Yang, W. Sima, X. Han, R. Wang, C. Jiang, W. Mao, P. Sun, "Failure analysis and maintenance of a surge capacitor on the neutral bus in a  $\pm 500$  kV HVDC converter station", IET Ren. Power. Generat., vol. 10, no 7, pp. 852-860, June 2016.
- [14] F. Yousef-Zai and D. O'Kelly, "Solid-state on-load transformer tap changer", Proc. Inst. Elect. Eng., vol. 143, no. 6, pp. 481-491, 1996.
- [15] S. Kouro, M. Malinowski, K. Gopakumar, J. Pou, L. G. Franquelo, B. Wu, et al., "Recent advances and industrial applications of multilevel converters", IEEE Trans. Ind. Electron., vol. 57, no. 8, pp. 2553-2580, Aug. 2010.
- [16] "IEEE Std. C37.2-2008", IEEE Standard Electrical Power System Device Function Numbers, Acronyms, And Contact Designations.
- [17] "IEEE Std. 519", IEEE Recommended Practices and Requirements for Harmonic Control in Electrical Power Systems.
- [18] V. Guerrero, J. Pontt, J. Dixon, J. Rebolledo, "A novel noninvasive failure-detection system for high-power converters based on scrs", IEEE Trans. Ind. Electron., vol. 60, no. 2, pp. 450-458, 2013.

- [19] P.W. Hammond, "Enhancing the reliability of modular medium voltage drives," IEEE Trans. Ind. Electron. vol. 49, no. 5, pp. 948-954, October 2002.
- [20] J. Rodriguez, P.W. Hammond, "Operation of a medium voltage drive under faulty conditions," IEEE Trans. Ind. Electron., vol. 52, no. 4, pp. 1080-1085, August 2005.
- [21] Infineon datasheet of the IGBT module, "FZ1200R17HE4P," published by Infineon Technologies AG, Germany, available online at: [www.infineon.com](http://www.infineon.com), edited in October 2016.
- [22] Thyristor-Based HVDC Transmission System (detailed model), published by MathWorks, available online at [www.mathworks.com](http://www.mathworks.com).
- [23] C. Liang, J. Xu, L. Luo, Y. Li, Qi Qi, P. Gao, Y. Fu, Y. Peng, "Harmonic elimination using parallel delta-connected filtering windings for converter transformers in HVDC systems", IEEE Trans. Power Del., vol. 32, pp. 933-941, 2017, ISSN 0885-8977.
- [24] M. O. Faruque, Y. Zhang, V. Dinavahi, "Detailed modeling of CIGRE HVDC benchmark system using PSCAD/EMTDC and PSB/SIMULINK", IEEE Trans. Power Del., vol. 21, no. 1, pp. 378-387, Jan. 2006.



**Daniel Legrand Mon-Nzongo** (S'2014) was born in Douala in 1986. He received B.S. and M.S. degrees (2010 and 2012) in Electrical Engineering from the University of Douala, Cameroon.

Since 2014, He is working toward the Ph.D. degree in the Department of Electrical Engineering and Automation of Fuzhou University, China. His current research interests include medium-voltage motor drives, harmonics interaction in large variable frequency drives

(VFDs) and grid-connected systems.



**Paul Gistain Ipoum-Ngome** (S'2017) was born in Douala in 1989. He received B.S. and M.S. degrees (2013 and 2015) in Electrical Engineering from the University of Douala, Cameroon. He also received the DEA in Electrical Engineering from the same university (2016).

Since September 2017, He is working toward the Ph.D. degree in the Department of Electrical Engineering and Automation of Fuzhou University, Fuzhou China. His current research

interests include high-power motor drives, harmonics interaction in variable frequency drives (VFDs) and grid-connected systems.



**Tao Jin** (M'2008) was born in Hubei province, China, in 1976. He received B.S. and M.S. degrees from Yanshan University respectively in 1997 and 2001, and the Ph.D. degree in Electrical Engineering from Shanghai Jiaotong University in 2005.

He has ever worked as research fellow in Virginia Polytechnic Institute and Imperial College London. Since 2009, He is a researching Professor in Fuzhou University. His current research interests include measurement

technology and new technologies in smart grid.



**Joseph Song-Manguelle** (M'07–SM'10) received the B.S. degree in pedagogical sciences and the M.S. degree in electrical engineering from the University of Douala, Cameroon, and the Ph.D. degree in electrical engineering from the Swiss Federal Institute of Technology, Lausanne, Switzerland, respectively in 1995, 1997 and 2004.

From 2004 to 2007, he held engineering positions with GE Global Research, Munich, Germany, and GE Oil and Gas, Le Creusot,

France, where he was involved in the design and test of large variable-frequency drives (VFDs), as well as developing new solutions for solving torsional vibration issues resulting from VFDs. In 2008, he joined GE Global Research, Niskayuna, NY, USA, where he designed high-voltage direct current power transmission and distribution systems for future long tieback subsea applications. In 2012, he joined ExxonMobil Development, Houston, TX as a Senior Electrical Engineer, where he was focused on oil and gas facilities design, as well as technical qualification of subsea electrical components such as subsea power cables, subsea VFDs, subsea motors (induction and permanent magnet), subsea transformers, and subsea switchgears. Since 2016, he has been assigned to Exxon Neftegas Limited, Yuzhno-Sakhalinsk, Russian Federation, where he is a Senior Electrical, Instrumentation and Controls Engineer, supporting ExxonMobil assets in Russia. In parallel to his industrial activities, since 2010 he is co-supervising Master's and Ph. D students in Douala University, Cameroon and at the University of Quebec, Trois-Rivières, QC, Canada.

Dr. Song-Manguelle is a member of the Petroleum and Chemical Industry Committee Standards and Marine Subcommittees, the Industrial Drives Committee, and the Power Electronics Committee of the IEEE Industry Applications Society. He currently serves as an Associate Editor of the Industrial Drives Committee for the IEEE TRANSACTIONS ON INDUSTRY APPLICATIONS.